

Polypropylene/Elastomer/Poly(styrene-co-acrylonitrile) Blends: Manifestation of the Critical Volume Fraction of SAN in Dynamic Mechanical, Tensile and Impact Properties

JAN KOLÁŘIK^{*1}, ALESSANDRO PEGORETTI², LUCA FAMBRI² and AMABILE PENATI²

1. *Institute of Macromolecular Chemistry, Academy of Sciences of the Czech Republic, 162 06 Prague 6, Czech Republic*

2. *Department of Materials Engineering, University of Trento, 38050 Trento, Italy*

Received January 11, 2000; revised February 14, 2000; accepted March 7, 2000

Abstract: The effect of the critical volume fraction v_{cr} of poly(styrene-co-acrylonitrile) (SAN) on the mechanical properties of its blends with rubber-toughened polypropylene (RTPP) containing about 12% grafted ethylene-propylene copolymer was studied. To encompass a wide spectrum of mechanical properties, blend components were selected which are characterized with rather different viscoelastic, tensile and ultimate properties. The SAN volume fraction in blends covers the interval 0~0.30; concentration dependencies of measured mechanical properties indicate $v_{cr} = 0.13$. Experimental data on storage modulus E_b' , loss modulus E_b'' , tensile modulus E_b , yield S_{yb} and tensile S_{ub} strength are in plausible accord with their simultaneous prediction based on a predictive scheme which operates with a two-parameter equivalent box model and the data on the phase continuity of components obtained from modified equations of the percolation theory. Strain at break, tensile energy to break and total impact energy of blends show a conspicuous drop in the interval 0~15 % of SAN where SAN forms a discontinuous component; further growth of the SAN fraction accounts for a reduction of the blend ultimate properties to the values typical of brittle polymers.

Keywords: Polymer blends, Critical volume fraction, Predictive models, Mechanical properties.

Introduction

The preparation of polymer blends is known to be a cost-effective way to upgrade existing polymers. As the potential application of candidate materials is frequently predetermined by their mechanical properties, it is desirable to anticipate at least some of the considered properties of intended blends as functions of their composition. At present, there exist various models which predict individual properties of composite systems consisting of a continuous matrix and one or more dispersed (discontinuous) components, e.g. modulus [1-3], yield or tensile strength [1,4,5] and permeability [6,7]. Such models could be applied to polymer blends, but only in the marginal composition intervals in which the

minority component is discontinuous. However, dispersed polymer components prone to creeping, yielding and plastic deformation are very different from inorganic fillers or reinforcements (showing "zero" compliance and plastic deformation), which are mainly used in composites. Recent studies [8-18] have shown that the minority component in two-component heterogeneous blends frequently assumes partial continuity at the critical volume fraction, as low as $0.1 < v_{cr} < 0.2$; as soon as $v > v_{cr}$, the minority component starts to affect blend properties relatively more than when it is in a fully dispersed state, i.e., at $v < v_{cr}$. In the central composition interval between the critical volume fraction of components v_{1cr} and v_{2cr} , phase structures with partially continuous constituents are typical of polymer

^{*}To whom all correspondence should be addressed.
Tel: 420-2-20403111; Fax: 420-2-367981
E-mail: office@imc.cas.cz

J. Polym. Res. is covered in ISI (CD, D, MS, Q, RC, S), CA, EI, and Polymer Contents.

blends. Obviously, the development of adequate predictive formats for selected mechanical properties of polymer blends and its experimental verification remain crucial problems in materials engineering. Proposed formats should allow for (i) the respective properties of components; (ii) a variety of phase structures, including those occurring in the interval of phase duality delimited by v_{1cr} and v_{2cr} ; and (iii) the strength of interfacial adhesion.

In our previous papers [10-15], we have proposed a predictive scheme for modulus E_b , yield strength S_{yb} (or tensile strength S_{ub}) and permeability P_b of polymer blends where the above mentioned requirements are respected. Experimental results show that physical properties of blends reflect v_{cr} in rather different ways. In general, the effect of v_{2cr} is the more visible, the higher value of a considered property displays the minority component 2 in comparison with the majority component 1. For example, electrical conductivity or permeability can be given for blends where minority components show values by several orders of magnitude higher than the majority components; v_{2cr} is then manifested as a "break" on the dependence property versus composition. Citing another example, if the differences between mechanical properties of glassy and/or crystalline blend constituents are smaller than one order of magnitude, the manifestation of v_{2cr} is less evident and its value can be adjusted by a fitting procedure. To encompass a wide spectrum of mechanical properties, we have selected model blends consisting of practically important polymers which differ in viscoelastic, tensile and ultimate properties: rubber-toughened polypropylene (RTPP) containing about 12% grafted ethylene-propylene copolymer (EPR) and poly(styrene-co-acrylonitrile) (SAN). As can be seen in the available literature [19-26], polyolefin blends with styrenics still attract much attention. The melt rheological behavior of PP/SAN blends (with 0-50% of SAN) was studied earlier [27] with the objectives of improving processability and of evaluating possible synergistic effects. Also in our blends, RTPP is the majority component, while the SAN weight fraction ranges between 0 and 0.33. The objective of this paper is to ascertain the effects of the transition from a solely particulate phase structure to a partly co-continuous phase structure on dynamic mechanical, tensile, and impact properties and to compare them, wherever possible, with existing model predictions. We have not used any compatibilizer in the RTPP/SAN blend preparation because it is known that compatibilizers may perceptibly affect the v_{cr} of components [25,28].

Experimental

1. Materials

Rubber-toughened polypropylene (RTPP), Moplen EPT30R (Montell, Ferrara, Italy), is a heterophase copolymer consisting of 88% of polypropylene and 12% of ethylene/propylene rubber (EPR) = 65/35 (density: 0.92 g/cm³). Poly(styrene-co-acrylonitrile) (SAN) Kostil B255 (Enichem, Mantova, Italy) is a copolymer containing about 24% of acrylonitrile (density: 1.07 g/cm³). The polymers were mixed in a Banbury mixer (chamber 4.3l; 164 rpm) at 175 °C for 3.5 min. The pellets produced were used for feeding a Negri-Bossi injection molding machine (barrel temperature: 235 °C; injection pressure: 200 bar) to produce test specimens for measurements of mechanical properties.

2. Test Methods

Ultrathin cryo-sections for microscopy were prepared by cutting the samples cooled to -130 °C. After collecting the sections on grids, staining in OsO₄ vapors was performed for 1 h. Scanning transmission electron micrographs were obtained using a scanning electron microscope with a transmission adapter (JSM 6400, JEOL).

Dynamic mechanical thermal analysis (DMTA) was performed in the interval from -150 to 200 °C (frequency: 1 Hz; heating rate: 3 °C/min.) by using the instrument PL-DMTA MkII produced by Polymer Laboratories, Loughborough, UK. A double cantilever was selected for the measurement of storage E' and loss E'' moduli (specimen dimensions: 40 mm × 10 mm × 4 mm; displacement: 0.032 mm).

An Instron Tester, type 4502, was used to measure the tensile mechanical properties of the studied blends. The tensile modulus was determined by using a strain gauge extensometer (Instron, model 2620; gauge length: 25 mm) on dog-bone shape specimens (gauge length: 80 mm; gauge cross-section: 10 mm × 4 mm) tested up to 1% strain at a cross-head speed of 1 mm/min. Tensile yield strength and strain, stress and strain at break, and tensile energy to break were ascertained on dog-bone specimens (gauge length: 60 mm; gauge cross-section: 12.8 mm × 3.3 mm) tested up to fracture at a cross-head speed of 5 mm/min.

Notched impact strength was measured with a Charpy instrumented pendulum CEAST, model 6549, on SENB specimens (width: 10 mm; thickness: 4 mm; notch depth: 5 mm) with the span length fixed to 40 mm. All impact tests were performed under the following experimental conditions: hammer weight: 2.5 Kg; striking speed: 1.513 m/s; data acquisition time: 64 ms; sampling time: 32 μs. On average, five test specimens were used for each

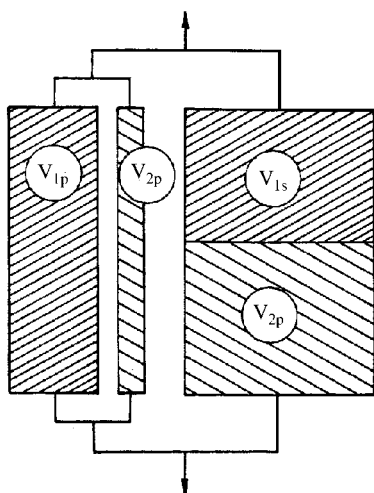


Figure 1. Equivalent box model for a binary blend 60/40 (schematically).

blend.

Predictive Scheme

Polymer blends are isotropic materials with three-dimensional continuity of one or more components so that simple parallel or series models or models for orthotropic or quasi-isotropic materials are not applicable. Our predictive scheme [10-15] is based on a combination of an equivalent box model (EBM) and the concept of phase continuity that involves the critical volume fractions of constituents. (It should be noted that "phase continuity" or "phase connectivity" may have different meaning in other papers.) The EBM in Fig. 1 operates with partly parallel (subscript p) and partly series (subscript s) couplings of components: fractions v_{1p} and v_{2p} form the parallel branch (being coupled in parallel to the acting stress), fractions v_{1s} and v_{2s} form the series branch (being coupled in series); these two branches, each consisting of two blocks, are coupled in parallel. The blocks in the EBM are presumed to have physical properties of the neat components; the application of the EBM is likely to fail if the mixing process produces a significant change in the structure and properties of a constituent. The EBM is a two-parameter model and of its four volume fractions v_{ij} only two are independent; its volume fractions are interrelated as follows:

$$\begin{aligned} v_p &= v_{1p} + v_{2p}; \quad v_s = v_{1s} + v_{2s}; \\ v_1 &= v_{1p} + v_{1s}; \quad v_2 = v_{2p} + v_{2s}; \\ v_1 + v_2 &= v_p + v_s = 1 \end{aligned} \quad (1)$$

In general, the EBMs are not self-consistent models; if they are intended for the prediction of physical properties of blends, the format requires two steps: (1) to derive the equations for the properties under consideration and (2) to calculate the volume fractions v_{ij} by using another appropriate model. (Obviously, these two steps are independent of each other.) In our previous papers [10-15], we have shown that v_{ij} can be evaluated by using modified equations rendered by the percolation theory [18, 29]. In this paper, the predictive scheme is used for simultaneous prediction of elastic modulus E_b , storage modulus E_b' , loss modulus E_b'' , yield strength S_{yb} and tensile strength S_{ub} . An essential feature of the proposed scheme is that all simultaneously predicted properties of a blend are related to a certain phase structure through an identical set of input parameters.

1. Equations for moduli and yield strength of binary blends in terms of the EBM

The tensile moduli of the parallel and series branches of the EBM are [10-12] the following: $E_p = (E_1 v_{1p} + E_2 v_{2p})/v_p$; $E_s = v_s / [(v_{1s}/E_1) + (v_{2s}/E_2)]$. The resulting tensile modulus of two-component systems is then given as the sum ($E_p v_p + E_s v_s$):

$$E_b = E_1 v_{1p} + E_2 v_{2p} + v_s^2 / [(v_{1s}/E_1) + (v_{2s}/E_2)] \quad (2)$$

Dynamic mechanical thermal analysis (DMTA) at a constant frequency offers the steady state harmonic conditions for which the elastic-viscoelastic correspondence principle is applicable [30]. Thus isochronous DMTA is a method allowing us to use the models for elastic materials and also for viscoelastic materials by replacing the elastic constants by complex (viscoelastic) counterparts [31,32]. Introducing $E_1^* = E_1' + iE_1''$, $E_2^* = E_2' + iE_2''$ and $E_b^* = E_b' + iE_b''$ into Eq.(2), we obtain

$$\begin{aligned} E_b' + iE_b'' &= (E_1' + iE_1'')v_{1p} + (E_2' + iE_2'')v_{2p} \\ &\quad + v_s^2 / [v_{1s}/(E_1' + iE_1'') + v_{2s}/(E_2' + iE_2'')] \end{aligned} \quad (3)$$

Hence

$$E_b' = E_1' v_{1p} + E_2' v_{2p} + v_s^2 N'/D \quad (4a)$$

$$E_b'' = E_1'' v_{1p} + E_2'' v_{2p} + v_s^2 N''/D \quad (4b)$$

where

$$N' = v_{1s} E_1' (E_2'^2 + E_2''^2) + v_{2s} E_2' (E_1'^2 + E_1''^2) \quad (5a)$$

$$N'' = v_{1s}E_1''(E_2'^2 + E_2''^2) + v_{2s}E_2''(E_1'^2 + E_1''^2) \quad (5b)$$

$$D = (v_{1s}E_2' + v_{2s}E_1')^2 + (v_{1s}E_2'' + v_{2s}E_1'')^2 \quad (5c)$$

"Perfect" adhesion between constituents and a linear stress-strain relationship indispensable for modulus measurements can be granted for glassy and/or crystalline polymers only at very low strains, typically below 1%, where virtually all blends show interfacial adhesion sufficient for transmission of the acting stress. At higher strains (usually 3-6%), the applied tensile stress is likely to exceed the linearity limit and to attain the value of yield strength, thus inducing yielding and plastic deformation of constituents. In our previous papers [10-12,15], we have derived the following equation for S_{yb} of the EBM visualized in Figure 1:

$$S_{yb} = S_{y1}v_{1p} + S_{y2}v_{2p} + AS_{y1}v_s \quad (6)$$

where $S_{y1} < S_{y2}$ characterize the parent polymers and A the extent of interfacial debonding. Two limiting values of S_{yb} , identified by the lower or upper bound, can be distinguished by means of Eq.(6): (i) Interfacial adhesion is so weak that complete debonding occurs before yielding between the fractions of constituents coupled in series ($A = 0$ at the yield stress). Consequently, the lower bound of S_{yb} is equal to the sum of the contributions of two parallel elements. (ii) Interfacial adhesion is strong enough to transmit the acting stress between constituents so that no debonding ($A = 1$) appears in the course of yielding; then the contribution of the series branch is added to that of the parallel branch (the effect of different strain rates in the parallel and series branches on S_{y1} and S_{y2} is neglected). However, if two components differing in yield strength are coupled in series, then the branch yields at S_{y1} or S_{y2} , whichever is lower. With regard to the previous studies showing [1,4] that formally identical equations of various types can be used for evaluation of the yield as well as the tensile strength of particulate systems, we have also tentatively applied [10-12] Eq.(6) for S_{ub} by replacing the yield strengths S_{y1} and S_{y2} by the tensile strengths S_{u1} and S_{u2} , respectively.

2. Calculation of the volume fractions in the EBM

The second step of the outlined scheme is the evaluation of v_{ij} defined in Figure 1. Percolation theory [29,33] provides a universal formula for the elastic modulus of binary systems where the contribution of the second component is negligible (analogous formulae hold for permeability and electrical conductivity [14,33,34]):

$$E_{1b} = E_0(v_1 - v_{1cr})^q \quad (7a)$$

where E_0 is a constant, v_{1cr} is the critical volume fraction (the percolation threshold) at which the component 1 becomes partially continuous and q is the critical exponent [29]. E_{1b} stands for the modulus of a "single-component" blend in which the component 1 assumes the same phase structure as in a blend with another polymer. Eq.(7a) has been experimentally shown [12,18] to plausibly fit the modulus of model blends with $E_1 \gg E_2$ in the range $v_{1cr} \leq v_1 \leq 1$, so that the modulus of the neat component 1 can be expressed as $E_1 = E_0(1 - v_{1cr})^{q_1}$. Thus

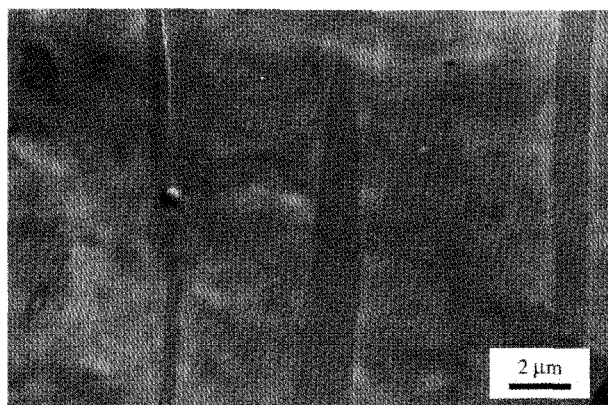
$$E_{1b} = E_1[(v_1 - v_{1cr})/(1 - v_{1cr})]^{q_1} \quad (7b)$$

If $E_1 \gg E_2$, the contribution E_2v_{2p} of that part of component 2 which is coupled in parallel and the contribution of the whole series branch (Figure 1) to the modulus of the EBM are negligible in comparison with the contribution E_1v_{1p} of component 1. Consequently, E_1v_{1p} (or E_2v_{2p} for $E_2 \gg E_1$) can be set equal to the apparent modulus E_{1b} (or E_{2b}), i.e., $E_{1b} = E_1v_{1p}$; $E_{2b} = E_2v_{2p}$. Comparing the latter relations with Eq. (7b), we can see that

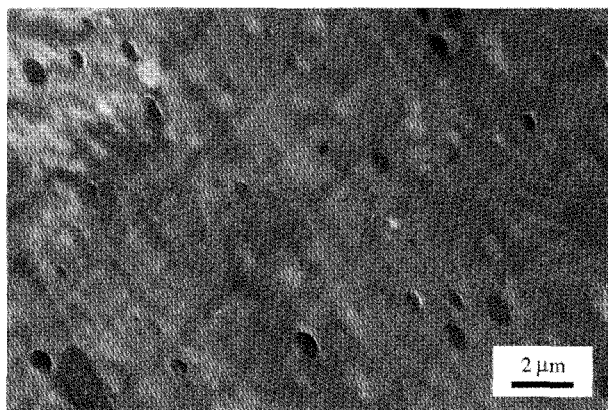
$$v_{1p} = [(v_1 - v_{1cr})/(1 - v_{1cr})]^{q_1}, \quad (8a)$$

$$v_{2p} = [(v_2 - v_{2cr})/(1 - v_{2cr})]^{q_2} \quad (8b)$$

The remaining v_{1s} and v_{2s} are evaluated by using Eq.(1). In the marginal zone $0 < v_1 < v_{1cr}$ (or $0 < v_2 < v_{2cr}$), where only component 2 (or 1) is continuous, simplified relations can be used for the minority component, i.e., $v_{1p} = 0$, $v_{1s} = v_1$ (or $v_{2p} = 0$, $v_{2s} = v_2$), to obtain an approximate prediction of mechanical properties. Most ascertained values of q are located in an interval of 1.6~2.0 so that $q = 1.8$ can be used also as an average value. For a three-dimensional cubic lattice, the percolation threshold $v_{cr} = 0.156$ was calculated [8,33,34]. In general, the patterns predicted by using "universal" values $v_{1cr} = v_{2cr} = 0.156$ and $q_1 = q_2 = 1.8$ should be viewed as a first approximation that may not be in good accord with experimental data because real v_{1cr} and v_{2cr} of polymer blends frequently differ from 0.156 and from each other. On the other hand, as soon as experimental data on physical properties of blends are available, actual values of the parameters can be adjusted by a fitting procedure. In this way, the EBM becomes a source of quantitative information on the phase duality of the blends studied (affected by relative viscosities, interfacial energy, processing conditions, phase structure coarsening, etc.).



(a)



(b)

Figure 2. Microphotographs of the phase structure of the RTPP/SAN = 85/15 blend. (a) along the direction of the injection molding and (b) across the direction of the injection molding.

Results and Discussion

The phase structure of RTPP/SAN blends is rather coarse as evidenced by Figure 2 for the blends containing 15% of SAN. In the direction along the injection molding (Figure 2(a)), gross "fibers" of SAN (dark color) can be seen; their imprints in the cross-section (Figure 2(b)) correspond to dark circles. These photographs evidence extensive orientation of the blend structure produced in the process of injection molding. White circles evenly distributed in gray areas (Figure 2(b)) obviously correspond to EPR domains embedded in PP. (As the EPR domains are fixed in the PP matrix, we will consider RTPP as a single component in the predictive scheme for binary systems.) A likely reason for the blend coarseness can be sought in a high interfacial energy of blended components (cf. ref. [35]). The microphotographs for other SAN concentrations are not presented because they do not allow us to determine the blend composition at which partial continuity of the SAN phase occurs.

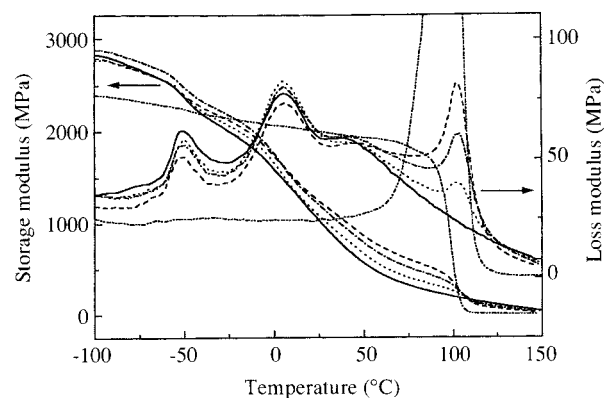


Figure 3. Effect of the composition (in weight %) of rubber-toughened polypropylene/poly(styrene-co-acrylonitrile) blends on the temperature dependence of the storage modulus E_b' and of the loss modulus E_b'' . RTPP/SAN = 100/0 (full line), 90/10 (dotted line), 80/20 (dash-and-dot line), 70/30 (dashed line), and 0/100 (dash-dot-dot line).

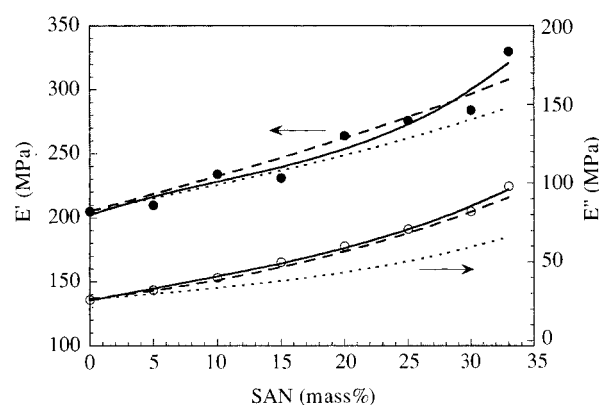


Figure 4. Effect of the composition (in weight %) of rubber-toughened polypropylene/poly(styrene-co-acrylonitrile) blends on the loss modulus E_b'' (SAN) and the storage modulus E_b' (SAN) read at the temperature of the SAN peak (around 100 °C). Experimental data: full lines. Prediction of Eqs. (4a) and (4b) for $v_{1cr} = 0.16$ and $v_{2cr} = 0.13$: "universal" $q_1 = q_2 = 1.8$ (dotted lines) and adjusted $q_1 = q_2 = 1.2$ (dashed lines).

To evaluate the v_{2cr} of SAN in the blends studied, it is necessary to analyze the effect of blend composition on measured mechanical properties (Figures 3-7). Inspecting Figures 4-7, we can see that (i) the experimental dependencies of S_{yb} and S_{ub} on blend composition start rising somewhat faster at $w_2 > 0.15$; (ii) the strain at break and tensile energy to break decrease rapidly with w_2 in the interval $0 < w_2 \leq 0.15$, while at $w_2 \geq 0.15$ they assume values similar to those for SAN. Thus for comparing experimental data with the prediction of the outlined format, we will consider $v_{2cr} = 0.13$, which corresponds to $w_{2cr} = 0.15$. Moduli E , E' , and E'' as functions of blend composition (Figures 4 and 5) do not show any visible "break" because the moduli of

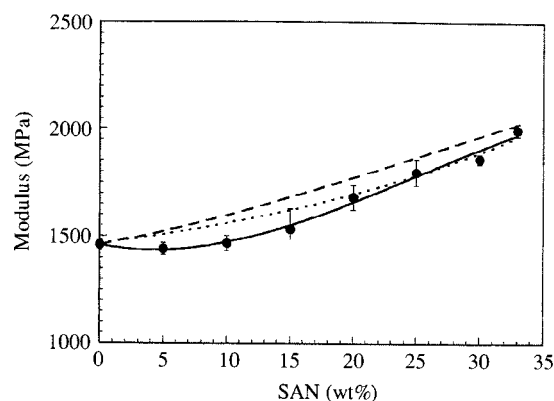


Figure 5. Effect of the composition (in weight %) of rubber-toughened polypropylene/poly(styrene-co-acrylonitrile) blends on tensile modulus E_b at 22 °C. Experimental data: full lines. Prediction of Eq.(2) for $v_{1cr} = 0.16$ and $v_{2cr} = 0.13$: "universal" $q_1 = q_2 = 1.8$ (dotted lines) and adjusted $q_1 = q_2 = 1.2$ (dashed lines).

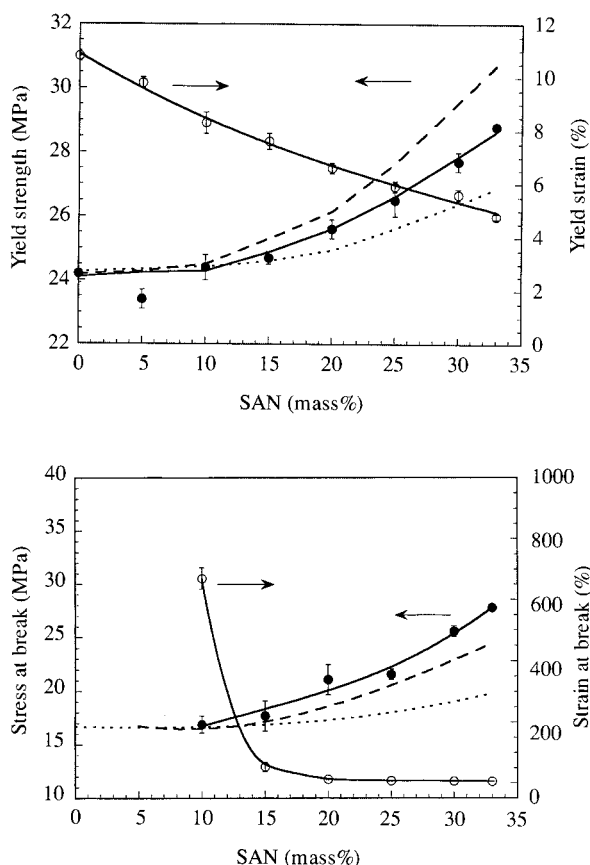


Figure 6. Effect of the composition (in weight %) of rubber-toughened polypropylene/poly(styrene-co-acrylonitrile) blends on (a) yield strength and yield strain and (b) stress at break and strain at break. Experimental data: full lines. Prediction of Eq. (6) for $v_{1cr} = 0.16$ and $v_{2cr} = 0.13$: "universal" $q_1 = q_2 = 1.8$ (dotted lines) and adjusted $q_1 = q_2 = 1.2$ (dashed lines).

blend components are not markedly different; in this case, $v_{2cr} = 0.13$ is confirmed by fitting experimental data points.

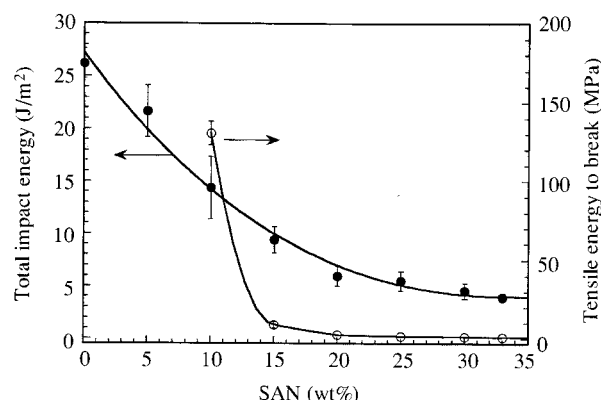


Figure 7. Effect of the composition (in weight %) of rubber-toughened polypropylene/poly(styrene-co-acrylonitrile) blends on their total impact energy and tensile energy to break. Experimental data: full lines (no predicted dependencies).

Dynamic mechanical patterns (Figure 3) of PP/SAN blends display three loss modulus peaks at about -50, 0 and 100 °C, which correspond to the glass transitions of the present components, i.e., EPR, PP and SAN, respectively (cf. ref. [36]). Temperature location of the PP or SAN peak is independent of the blend composition, which corroborates the presumed immiscibility of the blend components. In agreement with this observation, no additional loss peak can be seen which might originate from an interphase [37]. Loss modulus dependencies show regular changes with an increasing fraction of SAN in blends: while the peak at 100 °C grows, the other two peaks are proportionally reduced. Moreover, loss modulus curves of blends intersect at about 45 °C; this "isosbestic point" is believed [39] to indicate the inverse proportionality of the relaxation processes present below and above this temperature. A storage modulus between 0 and 100 °C rises in proportion to the SAN fraction in blends. Interestingly enough, T_g of EPR slightly decreases with the rising fraction of SAN in blends. The T_g depression can be explained [38] as a consequence of the negative compression (acting on particles of EPR) developed in the course of cooling the melt because EPR particles shrink more (being in the rubber-like state down to $T_g = -50$ °C) than PP ($T_g = 0$ °C) and SAN ($T_g = 100$ °C) particles. The increasing fraction of SAN in the blends enlarges an "average" temperature interval in which the negative pressure is built up.

E_b'' (SAN) equal to the height of the SAN loss modulus peak and corresponding E_b' (SAN) read at the peak temperature are confronted with the prediction of Eq.(4) in Figure 4. These quantities are expected to be sensitive to the changes in the SAN phase continuity in the series of blends. Interestingly enough, even a fraction of SAN as low as 5%

gives rise to a detectable peak at 100 °C, which clearly showing the sensitivity of DMTA. The calculated dependencies of E_b'' (SAN) and E_b' (SAN) are distinctly lower than the experimental data if the "universal" values $q_1 = q_2 = 1.8$ are used in Eqs. (8); however, the model fits the experimental data quite well if $q_1 = q_2 = 1.2$ are adjusted. On the other hand, the experimental data on tensile modulus E_b (22 °C) are lower than those predicted for $q_1 = q_2 = 1.8$ or $q_1 = q_2 = 1.2$ (Figure 5). The discrepancy at $w_2 \leq 0.15$ is brought about by the fact that the experimental values of E_b (22 °C) do not rise with the SAN fraction but are approximately equal to the value found for RTPP. For $w_2 > 0.15$, the accord between the experiment and the EBM improves.

The experimental data on the yield strength of blends (Figure 6(a)) are situated between two curves calculated with $q_1 = q_2 = 1.8$ or $q_1 = q_2 = 1.2$ by using Eq.(6) with $A = 1$. Obviously, as soon as the SAN phase assumes partial continuity at $w_{2cr} = 0.15$, the term $S_{y2}v_{2p}$ in Eq.(6) accounts for an increase in S_{yb} . On the other hand, the yield strain displays a monotonic decrease with w_2 without exhibiting any "break" at w_{2cr} . Experimental data on the tensile strength S_{ub} of blends (Figure 6(b)) depend on the blend composition in a way similar to S_{yb} . As the values of S_{ub} for PP and the 95/5 blend were not determined (corresponding strain at break was beyond the Instron Tester scale), the manifestation of v_{2cr} is indistinct. Equation (6) predicts lower values of S_{ub} for both $q_1 = q_2 = 1.8$ and $q_1 = q_2 = 1.2$, probably because the fracture mechanisms in PP and SAN are very different and the simplifying assumption neglecting different strain rates in parallel and series branches of the EBM is not valid. In our previous papers [10-15] we have found "universal" values $q_1 = q_2 = 1.8$ suitable for fitting experimental data on various heterogeneous blends. Figures 4-6 show that the EBM fits the experimental data on the RTPP/SAN blends better if $q_1 = q_2 = 1.2$ are used. A probable reason for this discrepancy might be sought in the rather strong orientation of the phase structure (Figure 2), which is no longer strictly isotropic.

Strain at break (Figure 6(b)) as well as tensile energy to break and notched impact strength (Figure 7) show a conspicuous drop in the interval $0 < w_2 \leq 0.15$; further growth of the SAN fraction accounts for the reduction in the blend extensibility and the impact resistance to the values typical of SAN. It is to be noted that the detrimental effect of SAN on the blend ultimate properties occurs in the interval where SAN forms a discontinuous component disrupting the phase continuity of RTPP, i.e., decreasing the value of v_{1p} . However, these mechanical

properties of blends can hardly be treated in terms of the EBM, so that there is no comparison possible between the experimental and theoretical data.

Conclusions

The effect of the critical volume fraction v_{2cr} (percolation threshold) of poly(styrene-*co*-acrylonitrile) (SAN) is manifested in the mechanical properties of its blends with rubber-toughened polypropylene (RTPP) containing about 12% grafted ethylene-propylene copolymer (the SAN volume fraction in blends ranges between 0 and 0.30). Experimental dependencies of storage modulus E_b' , loss modulus E_b'' , tensile modulus E_b , yield S_{yb} or tensile S_{ub} strength are in plausible accord with their simultaneous prediction based on a proposed predictive scheme operating with a two-parameter equivalent box model and data on the partial phase continuity of components obtained from modified equations of the percolation theory. The format considering polymer blends as isotropic materials with three-dimensional continuity of components allows for (i) the respective properties of components, (ii) phase structures encompassing the interval of phase duality delimited by the critical volumes of components, and (iii) the strength of interfacial adhesion. On the other hand, strain at break, tensile energy to break, and total impact energy of blends show a conspicuous drop in the interval 0-15% of the SAN where SAN forms a discontinuous component disrupting the phase continuity of RTPP. Further growth of the SAN fraction accounts for their reduction to the values typical of brittle polymers. A refined model accounting for profoundly differing values of the extensibility of RTPP and SAN would be necessary for better fitting experimental data.

Acknowledgment

The first author is greatly indebted to the Grant Agency of the Academy of Sciences of the Czech Republic for financial support of this work (Grant No. A4050706). The authors are grateful to Dr. P. Goberti and Mr. G. Vecchiattini (Montell, Ferrara, Italy) for supplying polypropylene and for the preparation of blends and test specimens.

References

1. L. E. Nielsen and R. F. Landel, *Mechanical Properties of Polymers and Composites*, M. Dekker, New

- York, 1994.
2. Z. Hashin, *Mechanics of Composite Materials*, F. Wendt, H. Liebowitz and N. Perone, Eds., Pergamon Press, New York, 1970.
3. S. McGee and R. L. McCullough, *Polym. Compos.*, **2**, 149 (1981).
4. L. Nicolais and M. Narkis, *Polym. Eng. Sci.*, **10**, 97 (1971).
5. B. Pukanszky, *Composites*, **21**, 255 (1990).
6. B. S. Mehta, A. T. DiBenedetto and J. Kardos, *J. Appl. Polym. Sci.*, **21**, 3111 (1977).
7. T. F. Blahovici and G. R. Brown, *Polym. Eng. Sci.*, **27**, 1611 (1988).
8. L. A. Utracki, *J. Rheol.*, **35**, 1615 (1991).
9. J. Lyngaae-Jorgensen and L. A. Utracki, *Makromol. Chem., Macromol. Symp.*, **48/49**, 189 (1991).
10. J. Kolařík, *Polym. Networks Blends*, **5**, 87 (1995).
11. J. Kolařík, *Eur. Polym. J.*, **34**, 585 (1998).
12. J. Kolařík, *Polym. Eng. Sci.*, **36**, 2518 (1996).
13. J. Kolařík and G. Geuskens, *Polym. Networks Blends*, **7**, 13 (1997).
14. J. Kolařík, L. Fambri, A. Pegoretti and A. Penati, *Polym. Eng. Sci.*, **40**, 127 (2000).
15. J. Kolařík, *J. Macromol. Sci., Phys.*, **39**, 53 (2000).
16. R. C. Willemse, A. Posthuma de Boer, J. van Dam and A. D. Gotsis, *Polymer*, **39**, 5879 (1998).
17. H. Veenstra, J. van Dam and A. Posthuma de Boer, *Polymer*, **40**, 1119 (1999).
18. J. Lyngaae-Jorgensen, A. Kuta, K. Sondergaard and K. V. Poulsen, *Polym. Networks Blends*, **3**, 1 (1993).
19. L. A. Utracki, *Commercial Polym. Blends*, Chapman & Hall, London, 1998.
20. L. A. Utracki, *Macromol. Symp.*, **118**, 335 (1997).
21. I. J. Hwang, M.H. Lee and B.K. Kim, *Eur. Polym. J.*, **34**, 671 (1998).
21. I. J. Hwang and B. K. Kim, *J. Appl. Polym. Sci.*, **67**, 27 (1998).
23. Z. Horak, J. Kolařík, M. Šípek, V. Hynek and F. Večerka, *J. Appl. Polym. Sci.*, **69**, 2615 (1998).
24. S. C. Tjong and S. A. Xu, *J. Appl. Polym. Sci.*, **68**, 1099 (1998).
25. S. A. Xu and C. M. Chan, *Polym. J.*, **30**, 552 (1998).
26. M. N. Bureau, E. DiFrancesco, J. Denault and J. I. Dickson, *Polym. Eng. Sci.*, **39**, 1119 (1999).
27. S. N. Maiti, V. Agarwal and A. K. Guipia, *J. Appl. Polym. Sci.*, **43**, 1891 (1991).
28. D. Bourry and B. D. Favis, *J. Polym. Sci., Polym. Phys.*, **36**, 1889 (1998).
29. P.G. De Gennes, *J. Phys. Lett. (Paris)*, **37**, L1 (1976).
30. R. M. Christensen, *Mechanics of Composite Materials*, Wiley, New York, 1979.
31. J. Kolařík, J. Janáček and L. Nicolais, *J. Appl. Polym. Sci.*, **20**, 841 (1976).
32. J. Kolařík, S. Hudeček, F. Lednický and L. Nicolais, *J. Appl. Polym. Sci.*, **23**, 1553 (1979).
33. W. Y. Hsu and S. Wu, *Polym. Eng. Sci.*, **33**, 293 (1993).
34. J. Sax and J.M. Ottino, *Polym. Eng. Sci.*, **23**, 165 (1983).
35. A. N. Wilkinson, L. Laugel, M. L. Clemens, V. M. Harding and M. Marin, *Polymer*, **40**, 4971 (1999).
36. Y. Feng, X. Jin and J. N. Hay, *J. Appl. Polym. Sci.*, **68**, 395 (1998).
37. H. Eklind and F. H. J. Maurer, *Polymer*, **37**, 2641 (1996).
38. J. Kolařík, G. L. Agrawal, Z. Kruliš and J. Kovář, *Polym. Compos.*, **7**, 463 (1986).
39. W. Dahl and F. H. Muller, *Z. Elektrochem.*, **65**, 652 (1961).